IEEE Access
Multidisciplinary ⋮ Rapid Review ⋮ Open Access Journal

Received April 3, 2020, accepted April 20, 2020, date of publication April 28, 2020, date of current version June 3, 2020.

Digital Object Identifier 10.1109/ACCESS.2020.2990970

Time-Delayed Control for Automated Steering Wheel Tracking of Electric Power Steering Systems

JAEMIN BAEK[1], (Member, IEEE), AND CHANGMOOK KANG[2], (Member, IEEE)
[1]Agency for Defense Development (ADD), The 1st R&D Institute–5th Directorate, Daejeon 34186, South Korea
[2]Department of Electrical and Engineering, Incheon National University (INU), Incheon 22012, South Korea

Corresponding author: Changmook Kang (mook@inu.ac.kr)

This work was supported by the Research Program (Improved Development of and Electric Power Steering System to enhance the driving stability of micro electric vehicles) funded by the Ministry of Trade, Industry and Energy (MOTIE), South Korea, under Grant 20007447.

ABSTRACT We present a time-delayed control (TDC) approach that applies it to the electric power steering (EPS) system for the first time. The TDC approach uses a one-sample delayed information of the system to cancel out uncertain and unknown dynamics, including disturbances. Therefore, it is possible to achieve the dominant pole using the pole-assignment so that it can be easily performed in the desired convergence rate. Moreover, given that tuning parameters of the TDC approach are very few in number, this control approach is very convenient for the practicing engineers who do not have control engineering knowledge. We proved the system criteria for the TDC approach applied to the EPS system and hence can always guarantee the system stability. The effectiveness of the TDC approach is verified through simulations, which is compared to that of the existing control approach.

INDEX TERMS Time-delayed control, steering control, electric power steering system.

I. INTRODUCTION

In recent years, interest in vehicles has been focused in which many researches allow for steering devices into vehicle fields. As one of the well-known steering devices, hydraulic power steering (HPS) system [1]–[3] has been applied to many vehicles, which has fast responsibility because it is implemented by mechanical way without electronic equipment. However, it may not only become decreased efficiency of the engine, but also may require regular management of the power oil. Additionally, given that this system requires a large number of equipments, it is not easy to guarantee spare space in vehicles.

As another power steering system, electronic power steering (EPS) system [4]–[6] has been developed to solve the problems of the HPS system. Given that the EPS system uses the electric battery to drive the motor, it aims at improving fuel efficiency of vehicles and does not require power oil replacement. Also, the number of equipments in the EPS system is less than that of HPS systems, and hence the EPS system allows enough space inside the vehicles. Moreover, this system has higher compatibility than the HPS system in eco-friendly vehicles such as electric vehicles. For these reasons, the EPS system is becoming more popular than the HPS system in modern vehicle fields. However, although the EPS system offers many advantages, it is difficult to design a control approach improving remarkable steering performance due to uncertainty and complexity of the system. Then, it may lead to a result that the undesirable steering performance holds the serious problem such as vehicle accident.

Many researchers have developed steering control approaches [7], [8] to avoid the above-mentioned problem while achieving the desired steering performance. A fixed-structure compensator control approach [7] has been adopted to the EPS system. Although this control approach is simple and easy to apply to the EPS system, it is susceptible to internal disturbances because it is strongly dependent on the EPS model. It implies that it may cause the system instability when the disturbances, *e.g.,* torque vibration, occur. Lead-lag compensator control approach [8] has been employed as a stabilizing compensator for loop shaping in the frequency domain. It can be observed that this control approach can reduce the adverse effects on torque vibration owing to the pole and zero gains. However, this control approach may not make a proper estimation in the dynamics behavior of

The associate editor coordinating the review of this manuscript and approving it for publication was Nasim Ullah.

the EPS system because it is hard to generate the dominant pole. It may yield a result in degrading the robustness of the EPS system.

Linear quadratic regulator control approach [9] has been designed as one of optimal control approaches. Its high gain parameters have made it possible to enhance the robustness in the EPS system. However, they may be sensitive to changes in the states of the system so that it may cause the undesirable side effects, e.g., steering vibration, in the EPS system. H-infinity control approaches [10], [11] have been also designed to enhance the robustness, which are adopted to obtain the optimal gains while reducing the disturbances. The optimal gains can be determined through some methods, including algebraic Riccati equation, mu-synthesis, and linear matrix inequality, and then they helps to provide a sense of stability for the steering of the autonomous vehicles. However, these control approaches require the complex procedures to obtain optimal gains, which have difficulty guaranteeing the optimal gains where there may not be global. They may cause a critical problem of losing the robustness due to abrupt and unsuspected disturbances, including undesirable input of the driver or uncertain components of road. Furthermore, given that all of control approaches introduced earlier should require the linearized EPS system which only exhibits dynamic characteristic near the operating point, it is hard to cope with the nonlinear elements of the EPS system.

Sliding-mode control approaches [12], [13] have been developed to remedy the above-mentioned problems, which are the well-known nonlinear control approaches. Sliding-mode observer approach [12] has been applied in the EPS system for reducing undesired side effects, including signal ripple. Conventional sliding-mode control approach [13] has been used to guarantee the robustness against the external disturbances. These control approaches can be easily applicable to the EPS system owing to the simplicity of their structure. However, despite these advantages, they require the exact information of the system model at all costs. In other words, the sliding-mode control approaches have no choice but to require accurate information of the EPS system model. It implies that improper control torque can be easily generated, which is directly related to the degraded steering performance in the EPS system.

As another view point, fuzzy control approaches [14]–[17] have been developed to be applied through work experience in the EPS system. Given that these fuzzy-based control approaches are based on membership functions which are designed into driving habits of the drivers, they do not require the information of the EPS system model. From these characteristics, it is easy to solve visual problems caused by operating the EPS system so that it has been very helpful to practicing engineers depending on the convenience. However, they have verified some benefits only for restricted driving environment, e.g., road with little impact on disturbance, and hence may not work well in several driving cases. To remedy these problems, wavelet fuzzy neural network control approach [18], genetic fuzzy control approach [19], and fuzzy neural sliding-mode control approach [20] have been introduced in the EPS system. Unfortunately, given that these control approaches should be required in a number of tuning parameters to estimate the system uncertainties, they are heavily dependent on many trial-and-error and time-consuming tasks due to parameters such as weighting factor. Furthermore, these control approaches may not guarantee convergence to the equilibrium point while stabilizing the EPS system. In this regard, it would be meaningful to design a simple, effective, and practical control approach while avoiding these complex problems in the EPS system.

In this paper, we first apply time-delayed control (TDC) approach to the EPS system. The TDC approach uses one-sample delayed information to cancel out uncertainties and disturbances of the system. Therefore, it is not required to know the information of the EPS system model. Moreover, this control approach is possible to achieve the dominant pole using the pole-placement term so that it can be easily performed in the desired convergence rate. Also, tuning parameters of the TDC approach are very few in number, and hence the TDC approach is very convenient for the practicing engineers who do not have control engineering knowledge. However, given that the TDC approach estimates the current states using one-sample delayed information of the system, the difference between the current and one-sample delayed information may make the errors which may cause the system instability. It can become feasible if the system stability can be always guaranteed. For this reason, the stability criteria for these errors is established in this paper so that the stability of the EPS system is guaranteed at all times. The effectiveness of the TDC approach is verified through simulation with the EPS system model, which is compared to that of the existing control approach.

The remainder of this paper is organized as follows: In Section II, we briefly introduce what the TDC approach is. Next, we explain the TDC approach using noise reduction method. In Section III, we carried out simulations with the EPS system. In Section IV, we conclude with a brief summary of this paper.

II. CONTROLLER DESIGN

A. TIME-DELAYED CONTROL

The nonlinear electric power steering (EPS) system [21], [22] can be expressed as follows:

$$\begin{aligned}\ddot{\boldsymbol{\theta}}_t^h &= \mathbf{f}(\boldsymbol{\theta}_t^h, \dot{\boldsymbol{\theta}}_t^h, \boldsymbol{\theta}_t^m, \mathbf{T}_t^d, \mathbf{T}_t^f) \\ &= -\bar{\mathbf{J}}_c^{-1}\big(\mathbf{K}_c\boldsymbol{\theta}_t^h + \mathbf{B}_c\dot{\boldsymbol{\theta}}_t^h - \frac{\mathbf{K}_c}{\mathbf{N}}\boldsymbol{\theta}_t^m - \mathbf{T}_t^d + \mathbf{T}_t^f\big) \qquad (1)\\ \ddot{\boldsymbol{\theta}}_t^m &= \mathbf{f}(\boldsymbol{\theta}_t^m, \dot{\boldsymbol{\theta}}_t^m, \boldsymbol{\theta}_t^h, \mathbf{T}_t^r, \mathbf{T}_t^e, \boldsymbol{\tau}_t^c) \\ &= \bar{\mathbf{J}}_{eq}^{-1}\big(\frac{\mathbf{K}_c}{\mathbf{N}}\boldsymbol{\theta}_t^h - \mathbf{K}_n\boldsymbol{\theta}_t^m - \mathbf{B}_{eq}\dot{\boldsymbol{\theta}}_t^m - \frac{\mathbf{R}_p}{\mathbf{N}}\mathbf{T}_t^r + \mathbf{T}_t^e + \boldsymbol{\tau}_t^c\big) \qquad (2)\end{aligned}$$

where

$$\bar{\mathbf{J}}_{eq} = \bar{\mathbf{J}}_m + \frac{\mathbf{R}_p^2\mathbf{M}_r}{\mathbf{N}^2}, \quad \mathbf{K}_n = \frac{\mathbf{K}_c + \mathbf{K}_r\mathbf{R}_p^2}{\mathbf{N}^2},$$

$$\mathbf{B}_{eq} = \mathbf{B}_m + \frac{\mathbf{R}_p^2 \mathbf{B}_r}{\mathbf{N}^2}$$

where $\boldsymbol{\theta}_t^h$, $\dot{\boldsymbol{\theta}}_t^h$, and $\ddot{\boldsymbol{\theta}}_t^h$ are steering wheel angle, steering wheel angular velocity, and steering wheel angular acceleration, respectively. $\boldsymbol{\theta}_t^m$, $\dot{\boldsymbol{\theta}}_t^m$, and $\ddot{\boldsymbol{\theta}}_t^m$ are motor position angle, motor angular velocity, and motor angular acceleration, respectively. $\mathbf{T}_t^d$, $\mathbf{T}_t^f$, $\mathbf{T}_t^r$, and $\mathbf{T}_t^e$ are driver torque, steering column friction torque, road reaction torque, and motor friction torque, respectively. $\bar{\mathbf{J}}_c$ and $\bar{\mathbf{J}}_m$ are steering column moment of inertia (MOI) and motor MOI, respectively. $\mathbf{B}_m$ and $\mathbf{B}_c$ are motor shaft viscous damping and steering column viscous damping, respectively. $\mathbf{K}_c$ and $\mathbf{K}_r$ are steering column stiffness and spring rate, respectively. $\mathbf{R}_p$ is steering column pinion radius. $\mathbf{N}$ is motor gear ratio. $\boldsymbol{\tau}_t^c$ is control input.

Solving for $\boldsymbol{\theta}_t^m$ in Eq. (2) yields

$$\boldsymbol{\theta}_t^m = \frac{1}{\mathbf{K}_n}\big(\bar{\mathbf{J}}_{eq}\ddot{\boldsymbol{\theta}}_t^m + \frac{\mathbf{K}_c}{\mathbf{N}}\boldsymbol{\theta}_t^h - \mathbf{B}_{eq}\dot{\boldsymbol{\theta}}_t^m - \frac{\mathbf{R}_p}{\mathbf{N}}\mathbf{T}_t^r + \mathbf{T}_t^e + \boldsymbol{\tau}_t^c\big) \tag{3}$$

Substituting Eq. (3) into Eq. (1), we have

$$\begin{aligned}\bar{\mathbf{J}}_c\ddot{\boldsymbol{\theta}}_t^h &= -\mathbf{K}_c\boldsymbol{\theta}_t^h - \mathbf{B}_c\dot{\boldsymbol{\theta}}_t^h + \mathbf{T}_t^d - \mathbf{T}_t^f \\ &\quad + \frac{\mathbf{K}_c}{\mathbf{K}_n\mathbf{N}}\big(-\bar{\mathbf{J}}_{eq}\ddot{\boldsymbol{\theta}}_t^m + \frac{\mathbf{K}_c}{\mathbf{N}}\boldsymbol{\theta}_t^h - \mathbf{B}_{eq}\dot{\boldsymbol{\theta}}_t^m - \frac{\mathbf{R}_p}{\mathbf{N}}\mathbf{T}_t^r + \mathbf{T}_t^e\big) \\ &\quad + \frac{\mathbf{K}_c}{\mathbf{K}_n\mathbf{N}}\boldsymbol{\tau}_t^c.\end{aligned} \tag{4}$$

When each side of Eq. (4) is multiplied by $\frac{\mathbf{K}_n\mathbf{N}}{\mathbf{K}_c}$ and summarized with $\bar{\mathbf{J}}_G\ddot{\boldsymbol{\theta}}_t^h$, Eq. (4) can be represented as follows:

$$\begin{aligned}\bar{\mathbf{J}}_G\ddot{\boldsymbol{\theta}}_t^h &= -\big(\frac{\bar{\mathbf{J}}_c\mathbf{K}_n\mathbf{N}}{\mathbf{K}_c} - \bar{\mathbf{J}}_G\big)\ddot{\boldsymbol{\theta}}_t^h \\ &\quad + \frac{\bar{\mathbf{J}}_c\mathbf{K}_n\mathbf{N}}{\mathbf{K}_c}\big(-\mathbf{K}_c\boldsymbol{\theta}_t^h - \mathbf{B}_c\dot{\boldsymbol{\theta}}_t^h + \mathbf{T}_t^d - \mathbf{T}_t^f\big) \\ &\quad + \frac{\mathbf{K}_c}{\mathbf{N}}\boldsymbol{\theta}_t^h - \bar{\mathbf{J}}_{eq}\ddot{\boldsymbol{\theta}}_t^m - \mathbf{B}_{eq}\dot{\boldsymbol{\theta}}_t^m - \frac{\mathbf{R}_p}{\mathbf{N}}\mathbf{T}_t^r + \mathbf{T}_t^e + \boldsymbol{\tau}_t^c\end{aligned} \tag{5}$$

When left side of Eq. (5) is summarized with $\ddot{\boldsymbol{\theta}}_t^h$, we obtain

$$\begin{aligned}\ddot{\boldsymbol{\theta}}_t^h &= -\bar{\mathbf{J}}_G^{-1}\big[\big(\frac{\bar{\mathbf{J}}_c\mathbf{K}_n\mathbf{N}}{\mathbf{K}_c} - \bar{\mathbf{J}}_G\big)\ddot{\boldsymbol{\theta}}_t^h\big] \\ &\quad + \bar{\mathbf{J}}_G^{-1}\big[\frac{\bar{\mathbf{J}}_c\mathbf{K}_n\mathbf{N}}{\mathbf{K}_c}\big(-\mathbf{K}_c\boldsymbol{\theta}_t^h - \mathbf{B}_c\dot{\boldsymbol{\theta}}_t^h + \mathbf{T}_t^d - \mathbf{T}_t^f\big)\big] \\ &\quad + \bar{\mathbf{J}}_G^{-1}\big[-\bar{\mathbf{J}}_{eq}\ddot{\boldsymbol{\theta}}_t^m + \frac{\mathbf{K}_c}{\mathbf{N}}\boldsymbol{\theta}_t^h - \mathbf{B}_{eq}\dot{\boldsymbol{\theta}}_t^m - \frac{\mathbf{R}_p}{\mathbf{N}}\mathbf{T}_t^r + \mathbf{T}_t^e\big] \\ &\quad + \bar{\mathbf{J}}_G^{-1}\boldsymbol{\tau}_t^c \\ &= \bar{\boldsymbol{\xi}}_t + \bar{\mathbf{J}}_G^{-1}\boldsymbol{\tau}_t^c\end{aligned} \tag{6}$$

where

$$\begin{aligned}\bar{\boldsymbol{\xi}}_t &= -\bar{\mathbf{J}}_g^{-1}\big[\big(\frac{\bar{\mathbf{J}}_c\mathbf{K}_n\mathbf{N}}{\mathbf{K}_c} - \bar{\mathbf{J}}_G\big)\ddot{\boldsymbol{\theta}}_t^h\big] \\ &\quad + \bar{\mathbf{J}}_G^{-1}\big[\frac{\bar{\mathbf{J}}_c\mathbf{K}_n\mathbf{N}}{\mathbf{K}_c}\big(-\mathbf{K}_c\boldsymbol{\theta}_t^h - \mathbf{B}_c\dot{\boldsymbol{\theta}}_t^h + \mathbf{T}_t^d - \mathbf{T}_t^f\big)\big] \\ &\quad + \bar{\mathbf{J}}_G^{-1}\big[-\bar{\mathbf{J}}_{eq}\ddot{\boldsymbol{\theta}}_t^m + \frac{\mathbf{K}_c}{\mathbf{N}}\boldsymbol{\theta}_t^h - \mathbf{B}_{eq}\dot{\boldsymbol{\theta}}_t^m - \frac{\mathbf{R}_p}{\mathbf{N}}\mathbf{T}_t^r + \mathbf{T}_t^e\big]\end{aligned}$$

where $\bar{\boldsymbol{\xi}}_t$ is not known to the users in the EPS system. $\bar{\mathbf{J}}_G$ is a positive constant that is called "TDC gain" in this paper.

For an estimation of $\bar{\boldsymbol{\xi}}_t$, we use an one-sample delayed information that is called time-delay estimation (TDE) [23], [24]. The estimation $\hat{\bar{\boldsymbol{\xi}}}_t$ is given as follows:

$$\hat{\bar{\boldsymbol{\xi}}}_t \cong \bar{\boldsymbol{\xi}}_{t-L} = \ddot{\boldsymbol{\theta}}_{t-L}^h - \bar{\mathbf{J}}_G^{-1}\boldsymbol{\tau}_{t-L}^c \tag{7}$$

where L is defined as a sampling time. $\bullet_{t-L}$ means one-sample delayed state of $\bullet_t$. From Eq. (7), time-delayed control (TDC) approach can be described as

$$\boldsymbol{\tau}_t^c = \underbrace{-\bar{\mathbf{J}}_G\ddot{\boldsymbol{\theta}}_{t-L}^h + \boldsymbol{\tau}_{t-L}^c}_{\text{TDE term}} + \underbrace{\bar{\mathbf{J}}_G\big(\ddot{\boldsymbol{\theta}}_{d,t}^h + \bar{\mathbf{K}}_1\dot{\mathbf{e}}_t^h + \bar{\mathbf{K}}_2\mathbf{e}_t^h\big)}_{\text{Pole-placement term}} \tag{8}$$

where $\mathbf{e}_t^h = \boldsymbol{\theta}_{d,t}^h - \boldsymbol{\theta}_t^h$ and $\dot{\mathbf{e}}_t^h = \dot{\boldsymbol{\theta}}_{d,t}^h - \dot{\boldsymbol{\theta}}_t^h$ are the steering wheel angle error and steering wheel angular velocity error, respectively. $\boldsymbol{\theta}_{d,t}^h$, $\dot{\boldsymbol{\theta}}_{d,t}^h$, and $\ddot{\boldsymbol{\theta}}_{d,t}^h$ are the desired steering wheel angle, desired steering wheel angular velocity, and desired steering wheel angular acceleration, respectively. $\bar{\mathbf{K}}_1$ and $\bar{\mathbf{K}}_2$ are positive constants for adjusting pole assignment. In Eq. (8), the first term, is called "TDE term", provides a remarkably close result to a continuous system if the sampling rate is faster than 30 times of its bandwidth [25] and hence L is set to be sufficiently small. The TDC approach in Eq. (8) can be depicted with a block diagram as shown in Figure 1.

Substituting Eq. (8) into Eq. (6) yields

$$\ddot{\mathbf{e}}_t^h + \bar{\mathbf{K}}_1\dot{\mathbf{e}}_t^h + \bar{\mathbf{K}}_2\mathbf{e}_t^h + \mathbf{E}_t = 0 \tag{9}$$

that is the error dynamics where $\mathbf{E}_t = \hat{\bar{\boldsymbol{\xi}}}_t - \bar{\boldsymbol{\xi}}_t$ is called "TDE error" in this paper. If $\bar{\mathbf{K}}_1 = 2\boldsymbol{\lambda}$ and $\bar{\mathbf{K}}_2 = \boldsymbol{\lambda}^2$ are set when $\mathbf{E}_t$ is bounded, Eq. (9) governs the error dynamics with a dominant pole where $\boldsymbol{\lambda}$ is a positive design value. To guarantee the upper bound value $\mathbf{E}^*$ of $\mathbf{E}_t$, *i.e.*, $|\mathbf{E}_t| \le \bar{\mathbf{E}}^*$, the TDC approach (Eq. (8)) should satisfy the following Lemma II-A.

Lemma 1: For a system model in Eqs. (1) and (2), the TDE error $\mathbf{E}_t$ *has the unknown upper-bound* $\bar{\mathbf{E}}^*$ *when the following stability criteria is satisfied as follows*:

$$\|1 - \boldsymbol{\Xi}^{-1}\bar{\mathbf{J}}_G\|_1 < 1$$

for time $t > 0$ *where* $\boldsymbol{\Xi} = \frac{\bar{\mathbf{J}}_c\mathbf{K}_n\mathbf{N}}{\mathbf{K}_c}$.

Proof: The proof is given in Appendix A. □

Remark 1: Stability criteria in Lemma 1 implies that $\bar{\mathbf{J}}_G$ *is upper-bounded to guarantee the system stability. Solving the inequality equation from the stability criteria, it means that the "TDC gain"* $\bar{\mathbf{J}}_G$ *should satisfy the following region:* $0 < \bar{\mathbf{J}}_G < \frac{2\bar{\mathbf{J}}_c\mathbf{K}_n\mathbf{N}}{\mathbf{K}_c}$.

B. NOISE REDUCTION METHOD

Given that the components of the EPS system are expensive, the one-sample delayed acceleration can be calculated by numerical differentiation as

$$\ddot{\boldsymbol{\theta}}_t^h = \frac{1}{L^2}\big(\boldsymbol{\theta}_t^h - 2\boldsymbol{\theta}_{t-L}^h + \boldsymbol{\theta}_{t-2L}^h\big). \tag{10}$$

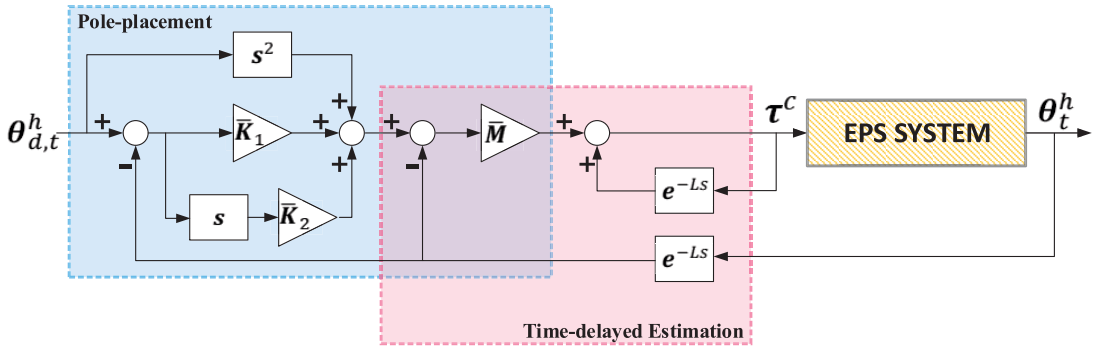

FIGURE 1. A block diagram of TDC approach.

Even if Eq. (10) holds a dominant aspect over the cost, the effect of the noise may be amplified due to numerical differentiation. To solve the above-mentioned problems, we introduce two solutions of the TDC approach as follows:

1) Using low value of $\bar{\mathbf{J}}_G$ in Eq. (8)

In Eq. (8), the TDC approach can be summarized as

$$\boldsymbol{\tau}^c_t = \boldsymbol{\tau}^c_{t-L} + \bar{\mathbf{J}}_G\big(-\ddot{\boldsymbol{\theta}}^h_{t-L} + \mathbf{u}_t\big) \tag{11}$$

where $\mathbf{u}_t = \ddot{\boldsymbol{\theta}}^h_{d,t} + \bar{\mathbf{K}}_1\dot{\mathbf{e}}^h_t + \bar{\mathbf{K}}_2\mathbf{e}^h_t$. When Eq. (11) is modified by a digital low-pass filter (LPF) with cutoff frequency $\boldsymbol{\lambda}$, it can be represented as

$$\bar{\boldsymbol{\tau}}^c_t = \bar{\boldsymbol{\tau}}^c_{t-L} + \frac{\bar{\mathbf{J}}_G\boldsymbol{\lambda}L}{(1+\boldsymbol{\lambda}L)}(-\ddot{\boldsymbol{\theta}}_{t-L} + \mathbf{u}_t) \tag{12}$$

where $\bar{\boldsymbol{\tau}}^c_t$ denotes the output torque generated by the LPF. As shown in Eq. (12), it is very similar to Eq. (11). In other words, the low value of $\bar{\mathbf{J}}_G$ provides the effect of a 1st-order LPF.

2) Using LPF directly in $\ddot{\boldsymbol{\theta}}^h_{t-L}$ of Eq. (8)

The TDC approach in Eq. (8) may generate the most amplified noise in $\ddot{\boldsymbol{\theta}}^h_{t-L}$. If the LPF is directly adopted in $\ddot{\boldsymbol{\theta}}^h_{t-L}$, the TDC approach can reduce the critical effect on the noise. The effectiveness of this approach will be confirmed through simulation in Section III.

III. SIMULATION

A. SETUP

A schematic diagram of the EPS system is described in Figure 2. To evaluate the effectiveness of the TDC approach, we conducted simulations with the EPS system model. The parameters of the EPS system model are chosen to be $\bar{\mathbf{J}}_c = 0.04$, $\bar{\mathbf{J}}_m = 0.004$, $\mathbf{B}_c = 0.072$, $\mathbf{B}_m = 0.0032$, $\mathbf{B}_r = 3820$, $\mathbf{K}_c = 115$, $\mathbf{K}_r = 81000$, $\mathbf{K}_t = 0.05$, $\mathbf{M}_r = 32$, $\mathbf{N} = 18.5$, $\mathbf{R}_p = 0.007$, and $L = 0.01$. L is given by the practical procedure introduced in Appendix B. The parameters of the TDC approach in Eq. (8) are set as $\bar{\mathbf{J}}_G = 0.003$, $\bar{\mathbf{K}}_1 = 40$, and $\bar{\mathbf{K}}_2 = 400$. Then, $\bar{\mathbf{J}}_G$ is chosen to be 0.003 so that Lemma II-A is computed to be 0.3412.

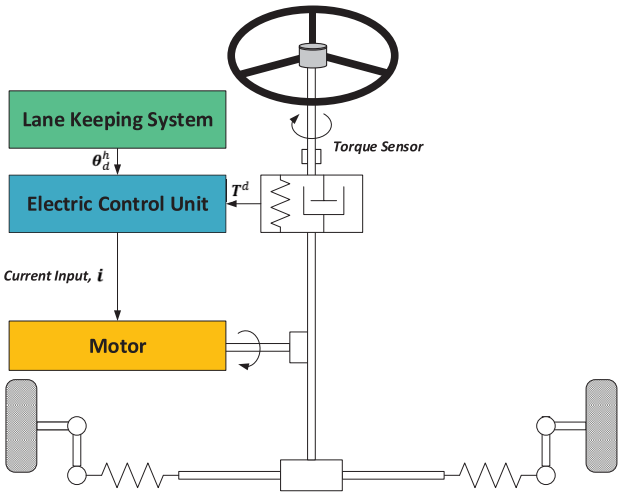

FIGURE 2. A schematic diagram of electric power steering (EPS) system.

B. DESCRIPTION

Lane keeping system (LKS) [22] helps in generating the desired steering wheel angle $\boldsymbol{\theta}^h_{d,t}$, as shown in Figure 2. The objective of this simulation is to make the steering wheel angle $\boldsymbol{\theta}^h_t$ follow the desired steering wheel angle $\boldsymbol{\theta}^h_{d,t}$, as shown in Figure 3. Two simulation scenarios are described as below:

- Sinusoidal response (Figure 3(a)):
  The sinusoidal reference trajectory is designed to be an actual driving situation on the highway. A driver torque is assumed as one of external disturbances, which is given in Figure 4. Additionally, the TDC approach is compared to the TDC approach with the LPF (TDC-LPF) which is based on noise reduction method introduced in Section II-B-2.
- Step response (Figure 3(b)):
  The step reference trajectory is designed to verify the convergence rate of the TDC approach through rising and settling time.

To demonstrate the performance of the TDC approach clearly, we have tried to choose the control approach in accordance with practical and theoretical aspects.

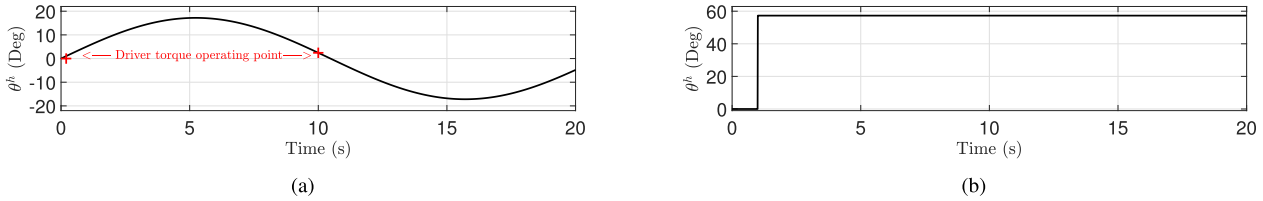

FIGURE 3. Steering wheel reference trajectory for automated motion in EPS system: (a) Sinusoidal reference trajectory. (b) Step reference trajectory.

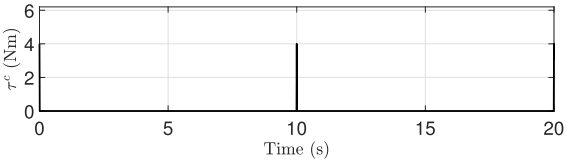

FIGURE 4. Driver torque generated in sinusoidal reference trajectory.

Then, a practical aspect implies that a control approach is of low complexity, computing implementable, and free of numerical problems when implemented. A theoretical aspect implies that a control approach does not require the knowledge of the system model. Therefore, the well-known proportional-integral-derivative control (PIDC) approach is employed for comparison, and its parameters are given in Appendix C. Next, to illustrate the benefit of the TDC-LPF approach introduced as an alternative to the TDC approach, the control input of the TDC approach is compared with that of the TDC-LPF approach. The simulation results are described in the Section III-C.

C. RESULTS

1) SINUSOIDAL RESPONSE

Figure 5 shows control torques of both the TDC approach and the TDC-LPF approach. Figure 5(a) represents the TDC approach which employs states using numerical differentiation as in Eq. (10). For this reason, it represents a result in the amplified noise such as signal ripple. On the other hand, as shown in Figure 5(b), the TDC-LPF approach uses the noise reduction method so that it can mitigate the mentioned problem. Moreover, it can be observed that the control input produces the stable and sufficient torques for reducing the undesired side effects generated by disturbance (Figure 4).

Figure 6 shows both steering errors and trajectories of the TDC approach and the PIDC approach in sinusoidal reference trajectory (Figure 3(a)). Figure 6(a) represents a comparison between the desired steering wheel angle and actual steering wheel angle. It is observed that the TDC approach provides better overall steering performance than the PIDC approach. It is a reason that the TDC approach makes an effort for achieving the dominant pole while canceling out the uncertain and unknown dynamics. Therefore, it helps to converge on the equilibrium point. On the contrary, the PIDC approach does not guarantee that the states converge to the equilibrium point. It represents a result in having the steering error boundedness, as shown in Figure 6(b). As another view point, these benefits of the TDC approach are significantly given as follows:

- Case 1) The vicinity of 0 s
- Case 2) The vicinity of 10 s.

In Case 1), the initial values of both desired steering wheel angular velocity and desired angular acceleration are not zero, as shown in Figure 3(a). Given that these can be recognized as external disturbances, all control approaches may also cause the large steering errors. However, it can be observed the TDC approach has an effort for converging quickly to the reference trajectory, unlike the PIDC approach. In Case 2), the external disturbances, *i.e.,* driver torque in Figure 4, are assumed to affect the EPS system. In other words, it means that the reference trajectory (Figure 3(a)) contains inherently the external disturbances which produce the large errors instantaneously. Despite these undesired side effects, the TDC approach provides enhanced robust steering performance, while the PIDC approach generates the degraded steering performance with the large oscillation. The root-mean-square (RMS) errors are given in Table 1.

TABLE 1. The RMS values of steering errors (sinusoidal response).

Control Strategies	Steering Angle (Deg)
PIDC	1.35
The proposed TDC	0.41

2) STEP RESPONSE

Figure 7 shows both steering errors and trajectories of the TDC approach and the PIDC approach in step reference trajectory (Figure 3(b)). Figure 7(a) represents a comparison between the desired steering wheel angle and actual steering wheel angle. It is observed that the TDC approach may instantaneously exhibit lower steering performance than the PIDC approach when the step input occurs at 1 s. It implies that the gain parameters tuned in the PIDC approach are set to be larger than those tuned in the TDC approach. This is why it can be identified as temporarily providing better steering performance. However, both rising time (@ 90%) and settling time (@ 3%) in the TDC approach are smaller than those in the PIDC approach. As a result, the TDC approach makes an effort of fast convergence to the equilibrium point, which offers better steering performance than the

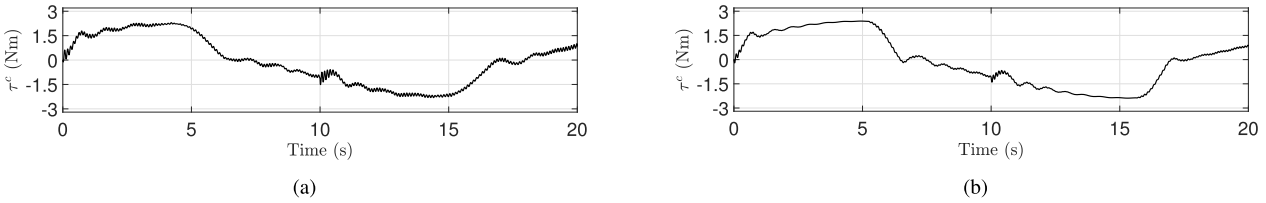

FIGURE 5. Comparison of control torques: (a) TDC approach. (b) TDC-LPF approach.

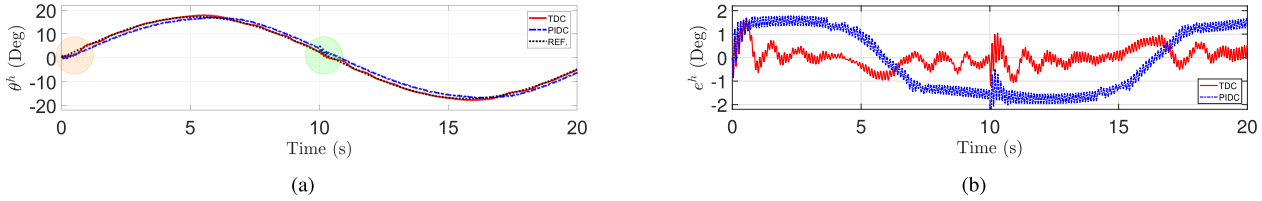

FIGURE 6. Comparison of PIDC approach (dotted-dashed line) and TDC approach (solid line): (a) Steering trajectories. (b) Steering errors.

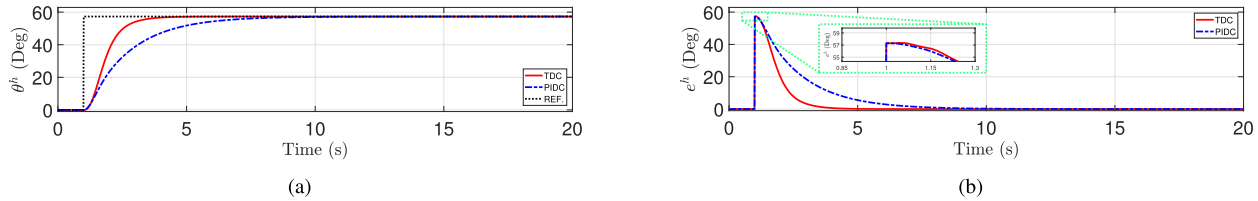

FIGURE 7. Comparison of PIDC approach (dotted-dashed line) and TDC approach (solid line): (a) Steering trajectories. (b) Steering errors.

TABLE 2. The RMS values of steering errors (step response).

Control Strategies	Steering Angle (Deg)
PIDC	13.15
The proposed TDC	9.02

TABLE 3. The rising and settling time (step response).

Control Strategies	Rising Time (s)	Settling Time (s)
PIDC	3.95	6.18
The proposed TDC	1.67	2.48

PIDC approach. Their results are described in Figure 7(b). The RMS errors and rising/settling time are given in Table 2 and Table 3, respectively.

IV. CONCLUSION

In this paper, we presented the TDC approach and first applied it to the EPS system. The TDC approach does not require the EPS system model. The dominant pole in the TDC approach could be easily set to improve the convergence rate significantly. We established the stability criteria such that the system stability can be guaranteed. From these benefits, the TDC approach improved steering performance while having a simple structure. The effectiveness of the TDC approach was confirmed through the simulations, which was compared with that of the well-known PIDC approach.

We believe that new control approaches based on the TDC approach can be applied to achieve more powerful steering performance in the EPS systems.

APPENDIXES

APPENDIX A
PROOF OF LEMMA 1

From Eq. (8), we can rearrange the TDC approach as follows:

$$\boldsymbol{\tau}_t^c = \boldsymbol{\tau}_{t-L}^c + \bar{\mathbf{J}}_G \boldsymbol{\omega}_t \tag{13}$$

where $\boldsymbol{\omega}_t = -\ddot{\boldsymbol{\theta}}_{t-L}^h + \ddot{\boldsymbol{\theta}}_{d,t}^h + \bar{\mathbf{K}}_1 \dot{\mathbf{e}}_t^h + \bar{\mathbf{K}}_2 \mathbf{e}_t^h$. Substituting Eq. (13) into Eq. (6) yields

$$\ddot{\boldsymbol{\theta}}_t^h = \bar{\boldsymbol{\xi}}_t + \bar{\mathbf{J}}_G^{-1} \boldsymbol{\tau}_{t-L}^c + \boldsymbol{\omega}_t. \tag{14}$$

Substituting Eq. (7) into Eq. (14), we have

$$\begin{aligned} \ddot{\boldsymbol{\theta}}_t^h &= \bar{\boldsymbol{\xi}}_t - \bar{\boldsymbol{\xi}}_{t-L} + \mathbf{u}_t \\ &= \mathbf{E}_t + \mathbf{u}_t \end{aligned} \tag{15}$$

where $\mathbf{u}_t = \ddot{\boldsymbol{\theta}}_{d,t}^h + \bar{\mathbf{K}}_1 \dot{\mathbf{e}}_t^h + \bar{\mathbf{K}}_2 \mathbf{e}_t^h$. $\mathbf{E}_t = \bar{\boldsymbol{\xi}}_t - \bar{\boldsymbol{\xi}}_{t-L}$ is the TDE error. When each side of Eq. (15) is multiplied by $\Xi = \frac{\bar{\mathbf{J}}_c \mathbf{K}_n \mathbf{N}}{\mathbf{K}_c}$, Eq. (15) can be represented as follows:

$$\Xi \ddot{\boldsymbol{\theta}}_t^h = \Xi \mathbf{E}_t + \Xi \mathbf{u}_t. \tag{16}$$

From Eq. (16), solving for $\mathbf{E}_t$ yields

$$\begin{aligned}\Xi\mathbf{E}_t &= \Xi\ddot{\boldsymbol{\theta}}_t^h - \Xi\mathbf{u}_t \\ &= \boldsymbol{\Lambda}_t + \boldsymbol{\tau}_t^c - \Xi\mathbf{u}_t \\ &= \boldsymbol{\Lambda}_t + \boldsymbol{\tau}_{t-L}^c - (\Xi - \bar{\mathbf{J}}_G)\mathbf{u}_t - \bar{\mathbf{J}}_G\ddot{\boldsymbol{\theta}}_{t-L}^h \qquad (17)\end{aligned}$$

where

$$\begin{aligned}\boldsymbol{\Lambda}_t = \frac{\mathbf{K}_n\mathbf{N}}{\mathbf{K}_c}\big(&-\mathbf{K}_c\boldsymbol{\theta}_t^h - \mathbf{B}_c\dot{\boldsymbol{\theta}}_t^h + \mathbf{T}_t^d - \mathbf{T}_t^f\big) \\ &- \bar{\mathbf{J}}_{eq}\ddot{\boldsymbol{\theta}}_t^m + \frac{\mathbf{K}_c}{\mathbf{N}}\boldsymbol{\theta}_t^h - \mathbf{B}_{eq}\dot{\boldsymbol{\theta}}_t^m - \frac{\mathbf{R}_p}{\mathbf{N}}\mathbf{T}_t^r + \mathbf{T}_t^e.\end{aligned}$$

The one-sample delayed information of the system dynamics is inserted in Eq. (17), we have

$$\begin{aligned}\Xi\mathbf{E}_t &= \boldsymbol{\Lambda}_t - \boldsymbol{\Lambda}_{t-L} + (\Xi - \bar{\mathbf{J}}_G)\dot{\boldsymbol{\theta}}_{t-L}^h - (\Xi - \bar{\mathbf{J}}_G)\mathbf{u}_t \\ &= \boldsymbol{\chi}_{1,t} + (\Xi - \bar{\mathbf{J}}_G)(\mathbf{E}_{t-L} + \mathbf{u}_{t-L}) - (\Xi - \bar{\mathbf{J}}_G)\mathbf{u}_t \\ &= \boldsymbol{\chi}_{1,t} + (\Xi - \bar{\mathbf{J}}_G)\mathbf{E}_{t-L} - (\Xi - \bar{\mathbf{J}}_G)(\mathbf{u}_t - \mathbf{u}_{t-L}) \\ &= (\Xi - \bar{\mathbf{J}}_G)\mathbf{E}_{t-L} + \boldsymbol{\chi}_{1,t} + \boldsymbol{\chi}_{2,t} \qquad (18)\end{aligned}$$

where $\boldsymbol{\chi}_{1,t} = \boldsymbol{\Lambda}_t - \boldsymbol{\Lambda}_{t-L}$ and $\boldsymbol{\chi}_{2,t} = -(\Xi - \bar{\mathbf{J}}_G)(\mathbf{u}_t - \mathbf{u}_{t-L})$ are considered as external terms which are bounded for a sufficiently small sampling time L according to the reasonable assumption, *i.e.,* $\| \bullet_t - \bullet_{t-L} \|_1 \leq \bar{\bullet}^*$ for a certain value $\bar{\bullet}^*$. By multiplying Eq. (18) by Ξ^{-1}, we have

$$\mathbf{E}_t = (1 - \Xi^{-1}\bar{\mathbf{J}}_G)\mathbf{E}_{t-L} + \boldsymbol{\chi}_t \qquad (19)$$

where $\boldsymbol{\chi}_t = \Xi^{-1}(\boldsymbol{\chi}_{1,t} + \boldsymbol{\chi}_{2,t})$ is also bounded. From Eq. (19), in the discrete-time domain, Eq. (19) can be represented as

$$\mathbf{E}(k) = \boldsymbol{\Psi}(k)\mathbf{E}(k-1) + \boldsymbol{\chi}(k). \qquad (20)$$

where $\boldsymbol{\Psi}(k) = 1 - \Xi^{-1}\bar{\mathbf{J}}_G$. Then, $\|\boldsymbol{\Psi}(k)\|_1 < 1$ is called "stability criteria" in this paper. In other words, if $\|1 - \Xi^{-1}\bar{\mathbf{J}}_G\|_1$ is less than 1, *i.e.,* $\|1 - \Xi^{-1}\bar{\mathbf{J}}_G\|_1 < 1$, Eq. (20) is asymptotically bounded with $\boldsymbol{\chi}(k)$, and hence $\mathbf{e}_t^h$ is always guaranteed to be bounded according to bounded-input-bounded-output stability [26]. Then, solving the inequality equation from the stability criteria, it implies that the TDC gain $\bar{\mathbf{J}}_G$ should be smaller than $\frac{2\mathbf{J}_c\mathbf{K}_n\mathbf{N}}{\mathbf{K}_c}$ to guarantee the system stability.

APPENDIX B
PRACTICAL WAY TO CHOOSE THE SAMPLING TIME

To begin with, suppose that the highest frequency component for a given analog signal is defined as $\mathbf{f}_{\max}$ in any systems. According to the Nyquist theorem, the sampling rate must be at least $2\mathbf{f}_{\max}$ or twice the highest analog frequency component of the control-loop in the systems. Actually, practicing engineers use a sampling rate of the control-loop in the systems that is 10 times the largest estimated or known frequency of the systems.

As shown in Figure 2, the LKS helps in generating the desired steering wheel angle $\boldsymbol{\theta}_{d,t}^h$, which provides it to the EPS system. Then, given that the LKS generates the desired steering wheel angle $\boldsymbol{\theta}_{d,t}^h$ through many sensors, including radar, laser imaging detection and ranging, camera, and ultrasonic wave, the sampling rate is limited in these sensors. For this reason, the LKS has a sampling rate with 10 Hz in industrial fields, and hence the practicing engineers use a sampling rate in the EPS system that is 10 times the largest estimated or known frequency in the LKS. From the basis mentioned above, we have considered the sampling rate with 100 Hz in this paper that means the sampling time with 0.01 s, *i.e.,* $L = 0.01$, in the EPS system.

APPENDIX C
PARAMETERS OF THE PIDC APPROACH

The parameters of the PIDC approach introduced in the Section III can be represented as follows:

- Proportional gain = 50
- Integral gain = 30
- Derivative gain = 0.05.

REFERENCES

[1] A. DellAmico and P. Krus, "Modeling, simulation, and experimental investigation of an electrohydraulic closed-center power steering system," *IEEE/ASME Trans. Mechatronics*, vol. 20, no. 5, pp. 2452–2462, Oct. 2015.

[2] W. Kemmetmuller, S. Muller, and A. Kugi, "Mathematical modeling and nonlinear controller design for a novel electrohydraulic power-steering system," *IEEE/ASME Trans. Mechatronics*, vol. 12, no. 1, pp. 85–97, Feb. 2007.

[3] W. Ribbens, *Understanding Automotive Electronics: An Engineering Perspective*. Oxford, U.K.: Butterworth-Heinemann, 2017.

[4] J.-H. Kim and J.-B. Song, "Control logic for an electric power steering system using assist motor," *Mechatronics*, vol. 12, no. 3, pp. 447–459, Apr. 2002.

[5] T. Yang, "A new control framework of electric power steering system based on admittance control," *IEEE Trans. Control Syst. Technol.*, vol. 23, no. 2, pp. 762–769, Mar. 2015.

[6] A. Badawy, J. Zuraski, F. Bolourchi, and A. Chandy, "Modeling and analysis of an electric power steering system," Soc. Autom. Eng., Int., Warrendale, PA, USA, SAE Tech. Paper 1999-01-0399, 1999.

[7] A. T. Zaremba, M. K. Liubakka, and R. M. Stuntz, "Control and steering feel issues in the design of an electric power steering system," in *Proc. Amer. Control Conference. (ACC)*, Dec. 1998, pp. 36–40.

[8] D. Lee, K.-S. Kim, and S. Kim, "Controller design of an electric power steering system," *IEEE Trans. Control Syst. Technol.*, vol. 26, no. 2, pp. 748–755, Mar. 2018.

[9] M. Parmar and J. Y. Hung, "A sensorless optimal control system for an automotive electric power assist steering system," *IEEE Trans. Ind. Electron.*, vol. 51, no. 2, pp. 290–298, Apr. 2004.

[10] X. Chen, T. Yang, X. Chen, and K. Zhou, "A generic model-based advanced control of electric power-assisted steering systems," *IEEE Trans. Control Syst. Technol.*, vol. 16, no. 6, pp. 1289–1300, Nov. 2008.

[11] R. Chabaan, "Control of electrical power assist systems: H_∞ design, torque estimation and structural stability," *JSAE Rev.*, vol. 22, no. 4, pp. 435–444, Oct. 2001.

[12] X. Li, X.-P. Zhao, and J. Chen, "Sliding mode control for torque ripple reduction of an electric power steering system based on a reference model," *Proc. Inst. Mech. Eng. D, J. Automobile Eng.*, vol. 222, no. 12, pp. 2283–2290, Dec. 2008.

[13] B. Chen, W. Hsu, and S. Huang, "Sliding-mode return control of electric power steering," Soc. Autom. Eng., Int., Warrendale, PA, USA, SAE Tech. Paper 2008-01-0499, 2008.

[14] J. E. Naranjo, C. Gonzalez, R. Garcia, T. dePedro, and R. E. Haber, "Power-steering control architecture for automatic driving," *IEEE Trans. Intell. Transp. Syst.*, vol. 6, no. 4, pp. 406–415, Dec. 2005.

[15] N. Vafamand, M. H. Asemani, A. Khayatiyan, M. H. Khooban, and T. Dragicevic, "TS fuzzy model-based controller design for a class of nonlinear systems including nonsmooth functions," *IEEE Trans. Syst., Man, Cybern. Syst.*, vol. 50, no. 1, pp. 233–244, Jan. 2020.

[16] X. Li, X.-P. Zhao, and J. Chen, "Controller design for electric power steering system using T-S fuzzy model approach," *Int. J. Autom. Comput.*, vol. 6, no. 2, pp. 198–203, May 2009.
[17] D. Saifia, M. Chadli, H. R. Karimi, and S. Labiod, "Fuzzy control for electric power steering system with assist motor current input constraints," *J. Franklin Inst.*, vol. 352, no. 2, pp. 562–576, Feb. 2015.
[18] Y.-C. Hung, F.-J. Lin, J.-C. Hwang, J.-K. Chang, and K.-C. Ruan, "Wavelet fuzzy neural network with asymmetric membership function controller for electric power steering system via improved differential evolution," *IEEE Trans. Power Electron.*, vol. 30, no. 4, pp. 2350–2362, Apr. 2015.
[19] L. Cai, A. B. Rad, and W.-L. Chan, "A genetic fuzzy controller for vehicle automatic steering control," *IEEE Trans. Veh. Technol.*, vol. 56, no. 2, pp. 529–543, Mar. 2007.
[20] F.-J. Lin, Y.-C. Hung, and K.-C. Ruan, "An intelligent second-order sliding-mode control for an electric power steering system using a wavelet fuzzy neural network," *IEEE Trans. Fuzzy Syst.*, vol. 22, no. 6, pp. 1598–1611, Dec. 2014.
[21] A. Marouf, M. Djemai, C. Sentouh, and P. Pudlo, "A new control strategy of an Electric-Power-Assisted steering system," *IEEE Trans. Veh. Technol.*, vol. 61, no. 8, pp. 3574–3589, Oct. 2012.
[22] W. Kim, Y. S. Son, and C. C. Chung, "Torque-Overlay-Based robust steering wheel angle control of electrical power steering for a lane-keeping system of automated vehicles," *IEEE Trans. Veh. Technol.*, vol. 65, no. 6, pp. 4379–4392, Jun. 2016.
[23] T. C. S. Hsia, T. A. Lasky, and Z. Guo, "Robust independent joint controller design for industrial robot manipulators," *IEEE Trans. Ind. Electron.*, vol. 38, no. 1, pp. 21–25, Feb. 1991.
[24] J. Baek, S. Cho, and S. Han, "Practical time-delay control with adaptive gains for trajectory tracking of robot manipulators," *IEEE Trans. Ind. Electron.*, vol. 65, no. 7, pp. 5682–5692, Jul. 2018.
[25] G. Franklin, J. Powell, and M. Workman, *Digital Control of Dynamic Systems*, vol. 3. Reading, MA, USA: Addison-Wesley, 1998.
[26] K. Hangos, J. Bokor, and G. Szederkényi, *Analysis and Control of Nonlinear Process Systems*, New York, NY, USA: Springer, 2006.

JAEMIN BAEK (Member, IEEE) received the B.S. degree in mechanical engineering from Korea University, Seoul, South Korea, in 2012, and the Ph.D. degree (M.S.–Ph.D. joint program) in creative IT engineering from the Pohang University of Science and Technology (POSTECH), in 2018.

Since 2018, he has been with Agency for Defense Development (ADD), Daejeon, South Korea. His main research interests include controller design for nonlinear control, adaptive/robust control, attitude control, gimbal, robotic, and satellite systems. He is a member of the IEEE Industrial Electronics Society, the IEEE Control Systems Society, and the Institute of Control, Robotics and Systems.

CHANGMOOK KANG (Member, IEEE) received the B.S. and Ph.D. degrees in electrical engineering from Hanyang University, Seoul, South Korea, in 2012 and 2018, respectively.

In 2018, he was with Agency for Defense Development (ADD), Daejeon, South Korea. He is currently an Assistant Professor with the Department of Electrical Engineering, Incheon National University (INU). His research interests include control theory, autonomous driving, machine learning, and system integration of intelligent vehicles. He is a member of the IEEE Intelligent Transportation Systems Society, the IEEE Control Systems Society, the Society of Automotive Engineers, the Korean Society of Automotive Engineers, and the Institute of Control, Robotics and Systems.